SUPPLEMENTAL METERIAL

Atomic Structures of Two Novel Immunoglobulin-Like Domain Pairs in the Actin Cross-Linking Protein Filamin

Outi K. Heikkinen, Salla Ruskamo, Peter V. Konarev, Dmitri I. Svergun, Tatu Iivanainen, Sami M. Heikkinen, Perttu Permi, Harri Koskela, Ilkka Kilpeläinen and Jari Ylänne

Fig. S1

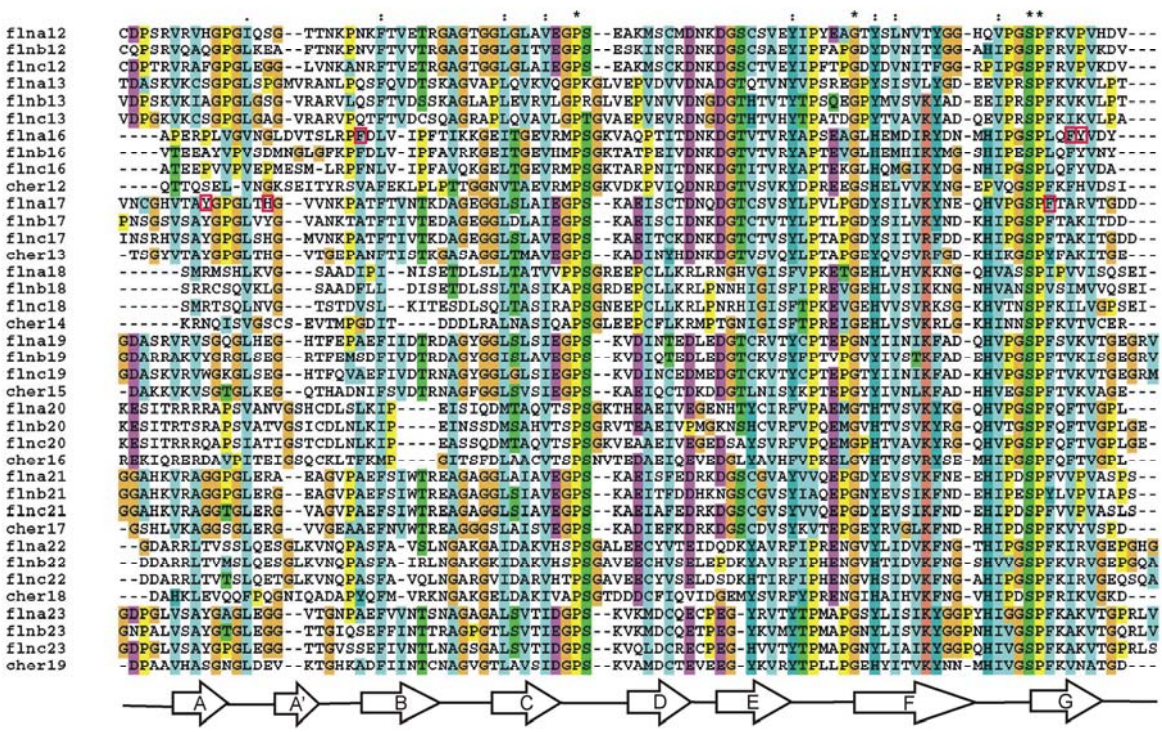

Fig. S1. Sequence Alignment of Human and *Drosophila melanogaster* IgFLNs

Sequences of human filamin A (accession code NM_001456), B (NM_001457) C (NM_001458) and *Drosophila melanogaster* (CG3937) IgFLNs were aligned by ClustalX 2.0 (Thompson et al. 1997). The A strand sequences of human IgFLNs 16, 18, 20 and corresponding sequences of *D. melanogaster* IgFLNs 12, 14 and 16 differ from other IgFLN A strands. Important aromatic amino acids (F1791, F1858, Y1859, Y1871, H1877 and F1948) in the IgFLNa16-17 interface have been highlighted by red rectangles.

Fig. S2

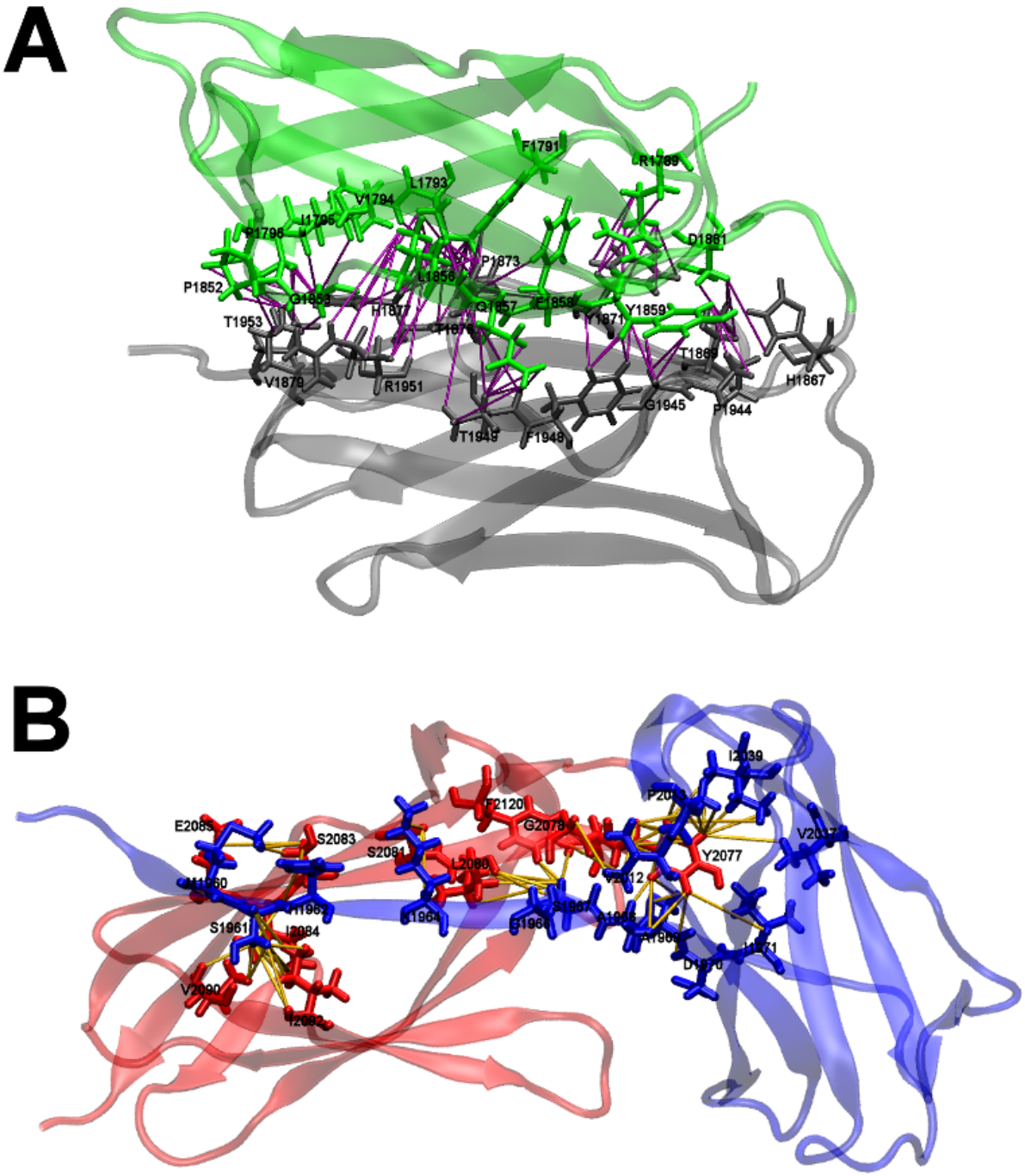

Fig. S2. Inter-Domain Distance Restraints of IgFLNa16-17 and IgFLNa18-19

The distance restraints that define the mutual orientation of the Ig domains of (A) IgFLNa16-17 (99 inter-domain NOEs) and (B) IgFLNa18-19 (76 inter-domain NOEs) are shown as purple and yellow lines, respectively. The residues housing the restraints are depicted as stick models and labeled with residue codes. Restraint visualization was done with VMD-XPLOR (Schwieters and Clore, 2001).

Fig. S3

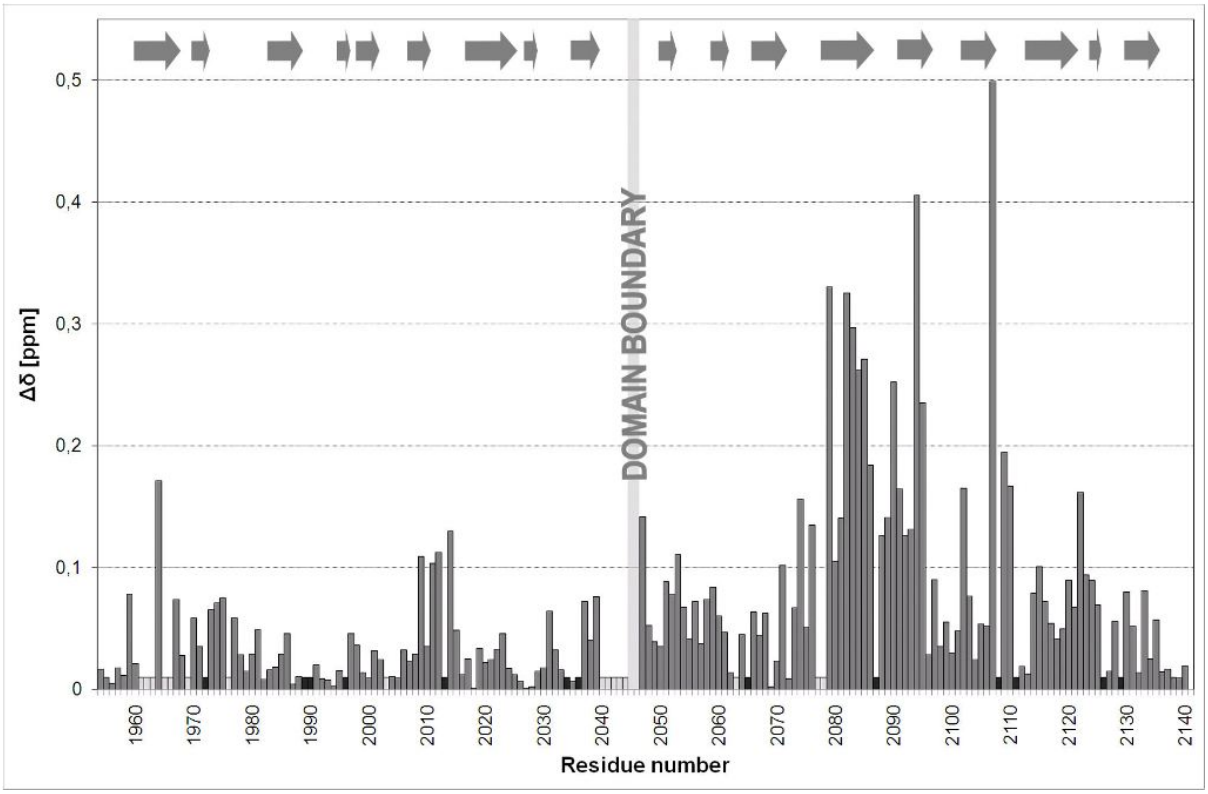

Fig. S3. Chemical Shift Mapping between IgFLNa18-19 and the Isolated Domains 18 and 19

Combined chemical shift differences of the backbone N-H signals (calculated as $((0.15*\Delta\delta_N)^2+(\Delta\delta_H)^2)^{½}$) between the double-domain IgFLNa18-19 and isolated single Ig domains 18 and 19 as function of residue sequence. Black bars represent prolines. The data is not available for residues marked with light gray due to missing or weak intensity ^{1}H-^{15}N-HSQC signals. The gray arrows represent the β-strands of IgFLNa18-19.

Fig. S4

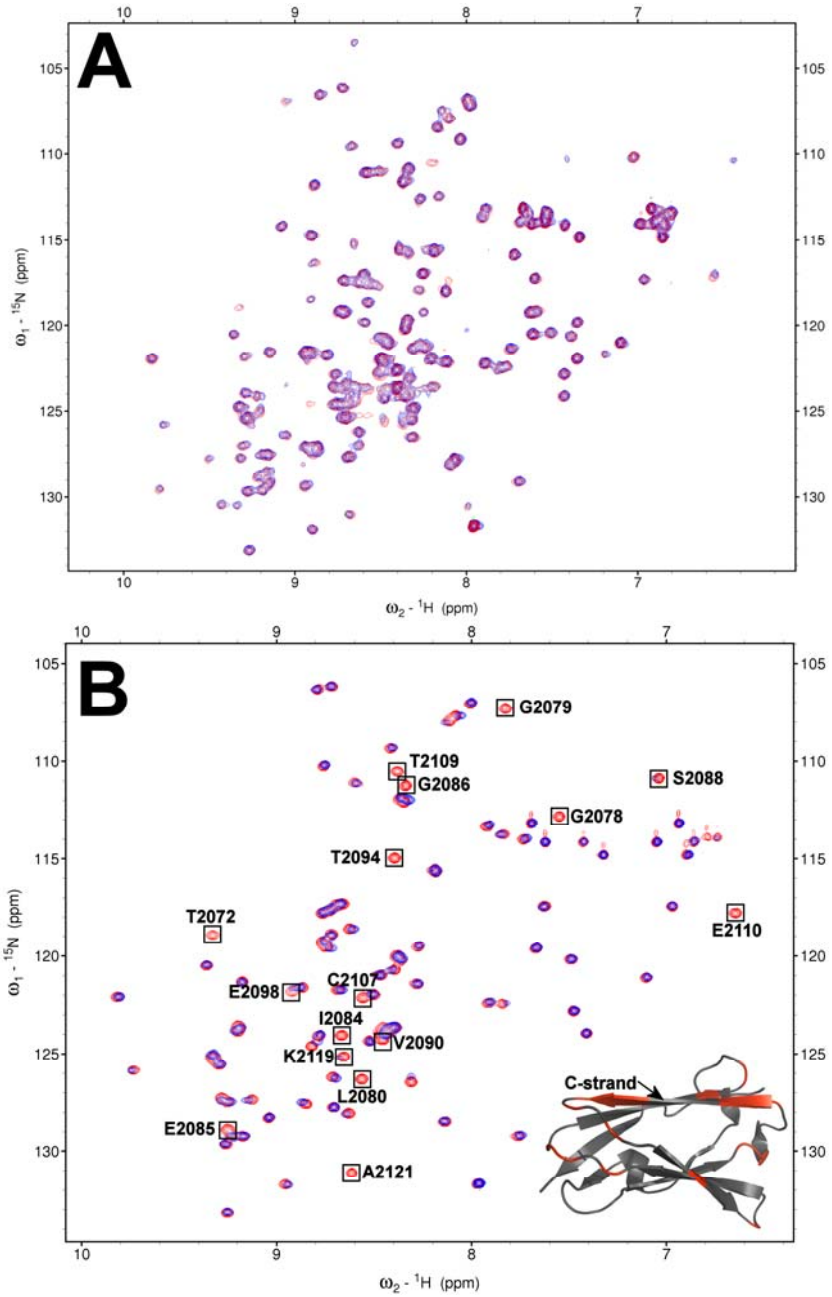

Fig.S4. IgFLNa18 Masks the Integrin β7 Binding Site in IgFLNa19

Integrin β7 peptide (Ac-^{776}PLYKSAITTTINP^{788}-NH_2) binding to β-strand C of IgFLNa19 is inhibited by IgFLNa18 in the double-domain. (A) ^{1}H-^{15}N-HSQC spectrum of IgFLNa18-19 without (red) and with 3.2-fold excess (blue) of integrin β7 peptide. Addition of integrin β7 peptide does not induce changes to the spectrum. (B) ^{1}H-^{15}N-HSQC spectrum of IgFLNa19 without (red) and with (blue) integrin β7 peptide (1:1 peptide-to-protein ratio). The spectrum changes markedly upon addition of the peptide which indicates binding of the peptide. Insert shows the structural location of the residues indicated in the spectrum with rectangles. Changes are at the CD face of IgFLNa19.

Fig. S5

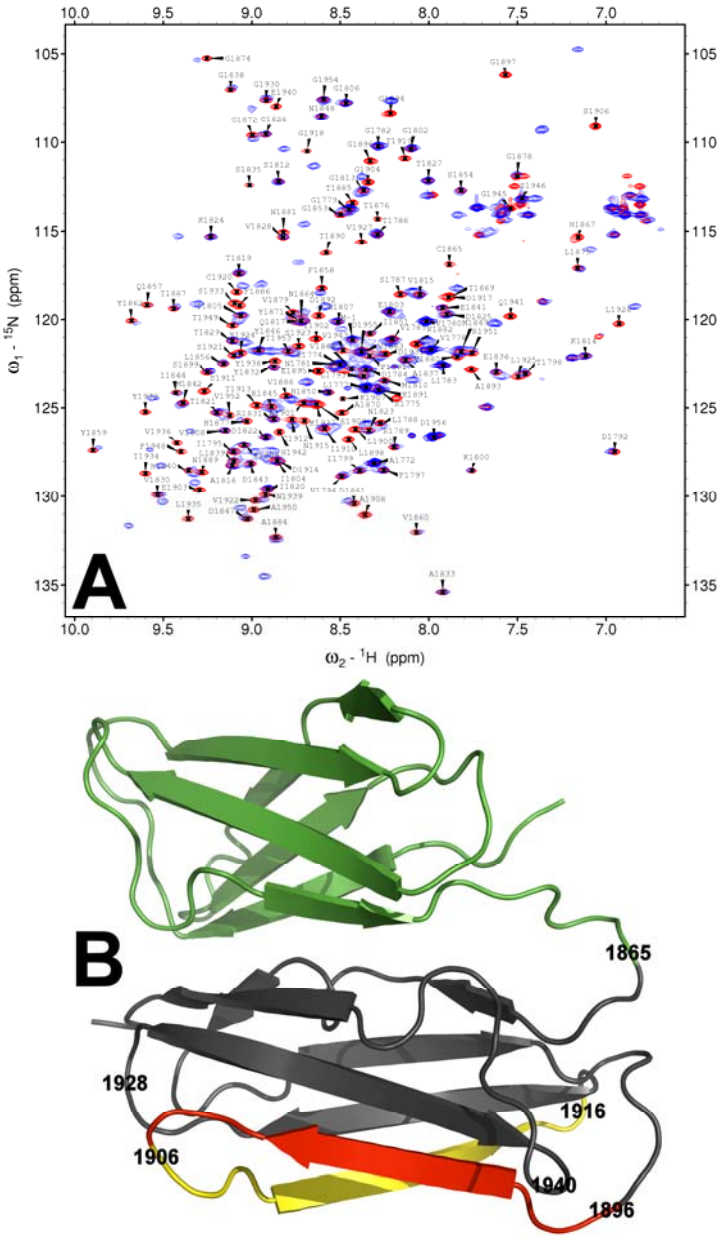

Fig S5. Glycoprotein Ibα Peptide Binds to the CD-Face of Domain 17 in the IgFLNa16-17 Construct.

Binding of GPIbα peptide (sequence ^{556}LRGSLPTFRSSLFLWVRPNGRV^{578}) to IgFLNa16-17 was confirmed with NMR titrations. (A) ^{1}H-^{15}N-HSQC spectrum of FLNa16-17 without (red) and with (blue) GPIbα peptide (1:1 peptide-to-protein ratio). Backbone amide signals are labeled with residue codes and sequence numbers The most pronounced spectral changes are situated at the CD face of domain 17 (residues 1896-1916). (B) The structure of IgFLNa16-17 highlighting the peptide binding site: Green–IgFLNa16; Gray–IgFLNa17; Red–C strand of IgLNa17; yellow–D strand of IgFLNa17. Certain sequence sites are indicated with sequence numbers to help structural mapping of the spectral changes.

Fig. S6

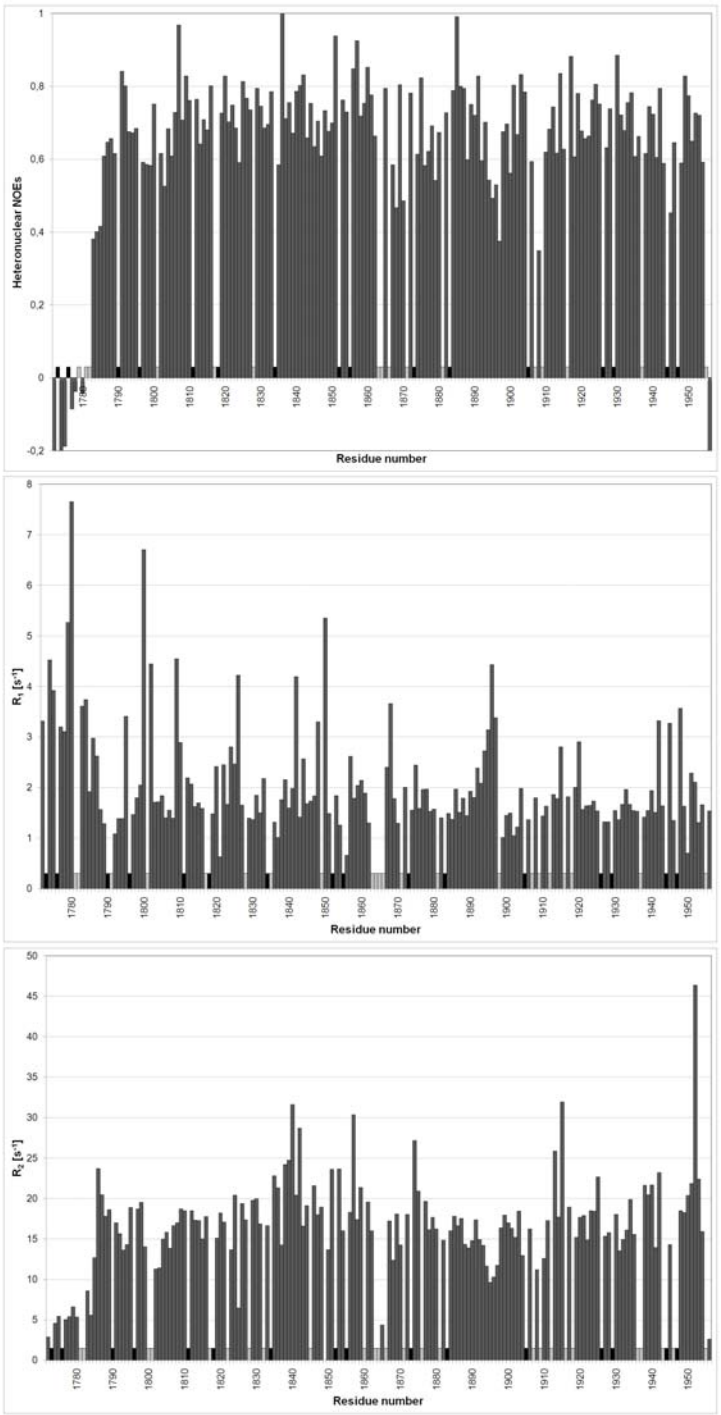

Figu. S6. Relaxation Parameters of IgFLNa16-17

Backbone amide ^{15}N relaxation rates and heteronuclear NOEs of IgFLNa16-17 as function of residue sequence. Black bars represent prolines. The data is not available for residues marked with light gray due to overlapping, missing or weak intensity ^{1}H-^{15}N-HSQC signals.

Fig. S7

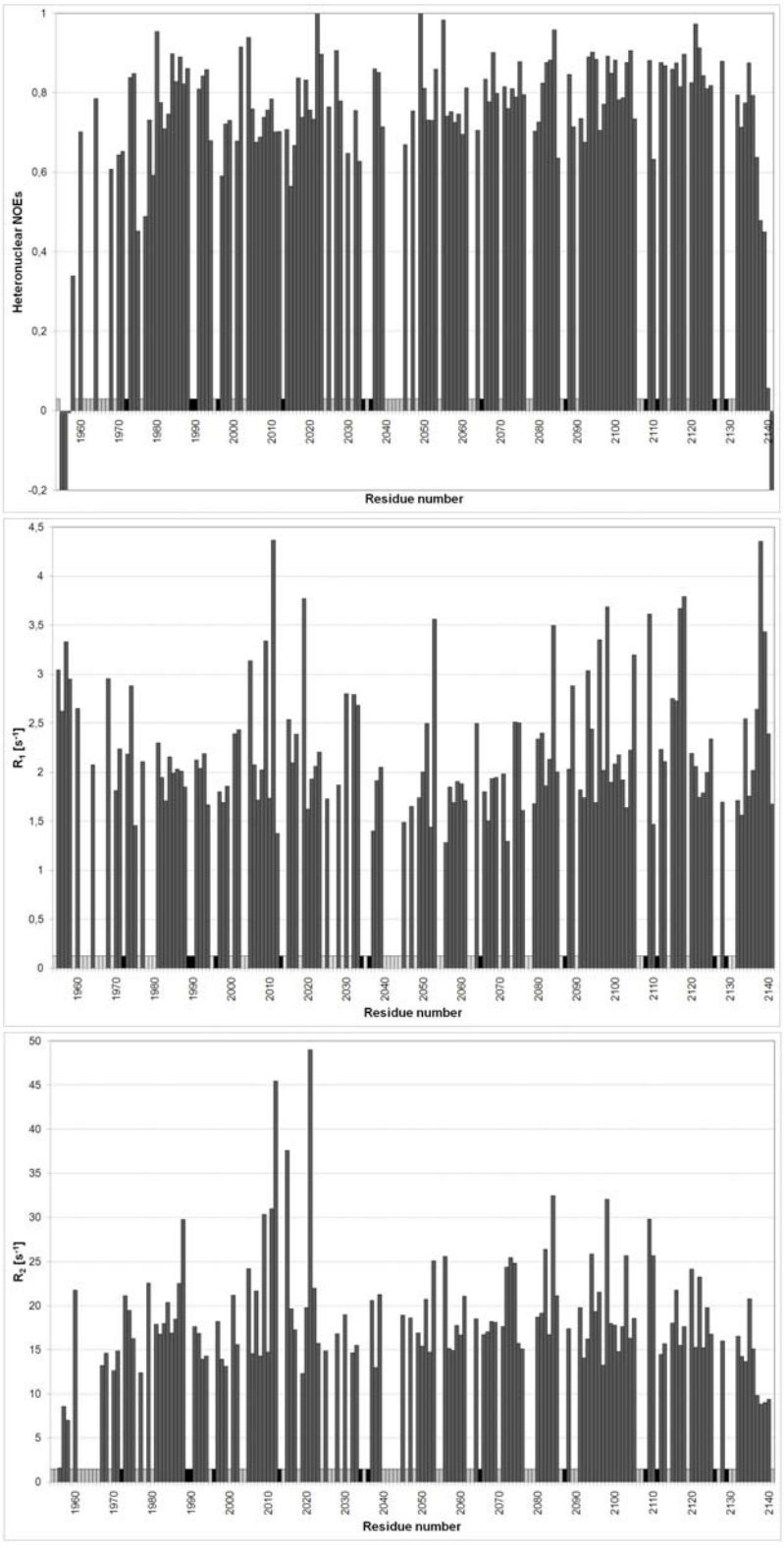

Fig. S7. Relaxation Parameters of IgFLNa18-19

Backbone amide ^{15}N relaxation rates and heteronuclear NOEs of IgFLNa18-19 as function of residue sequence. Black bars represent prolines. The data is not available for residues marked with light gray due to overlapping, missing or weak intensity ^{1}H-^{15}N-HSQC signals.

SUPPLEMENTAL METHODS

Structure Determination of IgFLNa16-17 and IgFLNa18-19

We have previously published essentially complete chemical shift assignments for IgFLNa16-17 and IgFLNa18-19 (Heikkinen et al., 2009). The details of IgFLNa16-17 and IgFLNa18-19 NMR samples used in structure determination can be found in this assignment note. EDTA was used in IgFLNa16-17 sample as protease inhibitior to prevent previously detected sample degradation during data acquisition. Addition of EDTA did not affect the chemical shifts of IgFLNa16-17. Chemical shift based backbone dihedral angle prediction with TALOS software (Cornilescu et al., 1999) yielded trustworthy values for 101 phi and 101 psi angles of IgFLNa16-17 and for 114 phi and 121 psi angles of IgFLNa18-19 and these were used as restraints in structure calculation. Based on the data from ^{13}C- and ^{15}N-edited NOESY-HSQC spectra the automatic NOESY assignment and structure calculation mode of CYANA 2.1 (Herrmann et al., 2002) generated 3439 and 2930 distance restraints for IgFLNa16-17 and IgFLNa18-19, respectively. In the structure ensemble of IgFLNa16-17 chosen for refinement the only restraint violation exceeding 0.5 Å for distances or 5° for angles was the Phi angle of Glu1940, in which the maximum violation was 5.5° whereas the IgFLNa18-19 structure ensemble contained no violations. Molecular dynamics refinement in implicit solvent yielded good quality structure ensembles and thus computationally more demanding refinement in explicit solvent was considered to be unnecessary, particularly since the preliminary trials did not seem to give any significant quality improvements. Quality indicators of the refined structure ensembles are presented in Table 2. WHAT CHECK (Hooft et al., 1996) (and PROCHECK-NMR (Laskowski et al., 1996) quality checks gave good scores and especially the Ramachandran diagram populations are excellent.

As the automated structure calculation protocol of CYANA occasionally failed to find inter-domain NOEs for the A-strand of IgFLNa18, which led to obscure progress of structure calculation, hydrogen bond restraints were set between the strand A of IgFLNa18 and strand C of IgFLNa19. The reason for the problems is obviously the shortage of backbone chemical shift assignments in the strand A (Heikkinen et al., 2009). Premising on manual NOE analysis 7 hydrogen bond constraints were set up between the backbone NH and CO groups of S1967-G2078, V1965-L2080, L2080-V1965, L1963-L2082, L2082-L1963, S1961-I2084 and I2084-S1961 (hydrogen bond donor listed first). After setting these restraints CYANA

repeatedly found numerous inter-domain NOE assignments and generated 42 distance restraints between the A strand of IgFLNa18 and the IgFLNa19 (Fig. S2B). Another way of dealing with the problem would have been manual assignment of the NOE cross-peaks, but we preferred the aforementioned procedure since it gives its own validation through automatically assigned NOEs and thus reveals potential operator made errors. Having used these somewhat artificial restraints we wanted to confirm that β-strand A indeed is bound to domain 19. Comparison of chemical shifts between IgFLNa18-19 and isolated single Ig domains 18 and 19 (Fig. S3) does not leave any question about the interaction interface. The largest chemical shift changes are located at the CD face of domain 19 where the strand A is bound. Unfortunately, there are many N-H signals missing at the strand A and thus the changes there are not so clearly revealed. Chemical shift assignment of isolated Ig domain 18 was carried out as described earlier (Heikkinen et al., 2009). The ^{1}H-^{15}N-HSQC resonance assignments of IgFLNa19 were kindly provided by Dr. Pengju Jiang and Dr. Iain Campbell, University of Oxford, UK. Heteronuclear NOEs (Fig. S7, see experimental details below) show that, except for the very terminal residues, IgFLNa18-19 does not contain floppy ends (or loops) which would have been manifested as low HetNOE values.

Titration of IgFLNa18-19 with Integrin β7 Peptide

Some features of the NMR spectra of IgFLNa18-19 indicated structural dynamicity in the A strand of the domain 18. Several backbone N-H correlations of the strand A were missing from the ^{1}H-^{15}N-HSQC spectrum of (Heikkinen et al., 2009) which posed some complications during structure determination. The CH_n signals were still visible in ^{1}H-^{13}C-HSQC and in ^{13}C-NOESY spectrum and gave the NOE information needed for structure determination. Disappearance of the backbone amides may reflect some kind of conformational exchange at the β-strand A. This implies that the interaction between the strand and the IgFLNa19 is not absolutely permanent but there is a chance for detachment. Displacement of β-strand A of IgFLNa20 from IgFLNa21 by integrin β7 peptide has been demonstrated earlier (Lad et al., 2007). Integrin β7 is also known to interact with IgFLNa19 (Kiema et al., 2006). Interaction between the integrin β7 peptide and β-strand C of IgFLNa19 was demonstrated using NMR titrations. We wanted to find out if integrin β7 peptide is also able to displace the β-strand A of IgFLNa18 from the CD face of IgFLNa19. We titrated 0.8 mM ^{13}C^{15}N-labeled IgFLNa18-19 sample (100 mM NaCl, 1 mM DTT, 2 mM NaN_3, 50 mM

sodium phosphate pH 6.8) with 5 mM integrin β7 peptide solution (in the same buffer as the protein sample) at 30 °C. Integrin β7 peptide (sequence Ac-^{776}PLYKSAITTTINP^{788}-NH_2), kindly provided by Dr. Pengju Jiang and Dr. Iain Campbell, University of Oxford, UK, was originally from EZBiolab (USA). ^{1}H-^{15}N-HSQC spectrum of IgFLNa18-19 was recorded at each titration point. The results of the titration are shown in Fig. S4A. ^{1}H-^{15}N-HSQC spectrum of IgFLNa18-19 did not show any changes on the course of titration which is an indication that IgFLNa18-19 does not strogly interact with integrin β7 peptide. We checked the interaction between integrin β7 peptide and ^{15}N-labelled IgFLNa19 under the same experimental conditions as was used in titration of IgFLNa18-19. The interaction between the isolated domain 19 and the integrin β7 peptide was seen clearly already with 1:1 peptide-to-protein ratios (Fig. S4B). Several ^{1}H-^{15}N-HSQC cross-peaks disappeared from the spectrum. All affected signals are located at or close to the CD face. These data imply that the presence of IgFLNa18 inhibits integrin β7 binding to IgFLNa19.

Titration of IgFLNa16-17 with Glycoprotein Ibα Peptide

IgFLNa17 has been previously shown to interact with glycoprotein Ibα (Nakamura et al., 2006). The interaction interface in the double-domain construct 16-17 is structurally very similar to the isolated domain 17 and the presence of domain 16 should not affect the interaction. We confirmed the GPIbα binding to IgFLNa16-17 with biochemical experiments (see the main text). We also checked the glycoprotein Ibα binding to IgFLNa16-17 using NMR titrations. 1 mM ^{13}C^{15}N-labeled IgFLNa16-17 sample (1 mM DTT, 2 mM NaN_3, 2mM EDTA, 50 mM sodium phosphate pH 6.8) was titrated with 5 mM GPIbα peptide solution in sample buffer at 30 °C. ^{1}H-^{15}N-HSQC spectrum of IgFLNa16-17 was recorded at each titration point. GPIbα peptide (sequence ^{556}LRGSLPTFRSSLFLWVRPNGRV^{578}) was chemically synthesized and purified by Tufts University Core Facility, Boston, USA. Results of the titration are shown in Fig. S5. Major changes were detected in the spectrum of IgFLNa16-17 upon peptide addition. The interaction was in the slow-exchange NMR time-scale. As expected, the most pronounced spectral changes were detected at the CD face of IgFLNa17. There were also relatively large changes in the other parts of IgFLNa17, which implies that, the peptide binding slightly molds the structure of the entire domain. Domain 16 did not exhibit substantial spectral changes. Detailed chemical shift mapping would have required complete reassignment of the domain 17. In conclusion, also NMR spectroscopic

experiments confirm that the presence of domain 16 does not interfere with GPIbα binding to IgFLNa17.

Backbone Amide Relaxation Rates and Heteronuclear NOEs of IgFLNa16-17 and IgFLNa18-19

The sample conditions in relaxation measurements were the same as in structure determination. All NMR relaxation experiments were run on Varian Inova 600 MHz spectrometer equipped with 5 mm z-gradient triple resonance probehead. The ^{15}N R_1 and R_2 relaxation rates of the backbone amide groups were measured using three-dimensional relaxation rate resolved ^{1}H-^{15}N-HSQC spectra (Heikkinen and Kilpeläinen, 2001; Koskela et al., 2004). Inverse Laplace transform was applied to the relaxation dimension of the three-dimensional datasets using GIFA software (Delsuc and Malliavin, 1998; Pons et al., 1996). The heteronuclear NOEs of the backbone amide nitrogens were determined using conventional methods (Farrow et al., 1994).

The relaxation rates and heteronuclear NOEs of IgFLNa16-17 and 18-19 are shown in Supplementary Figs. S5 and S7, respectively. The data for several residues of IgFLNa18-19 and some residues of IgFLNa16-17 are missing due to weak, absent or overlapping ^{1}H-^{15}N-HSQC signals. The relaxation data shows that all the domains are tightly folded except for the termini of the chains. There do not seem to be any particularly flexible loops in the structures. The relaxation properties confirm that the N-terminal residues of IgFLNa16-17 (1772-1785) corresponding to predicted A-strand are unstructured. In both domain pairs the relaxation properties of the domains are similar which implies that the domains tumble in solution as a single uniform unit. We decided to omit the more elaborate modelfree analysis of the data and determination of generalized order parameters since there is quite a lot of data missing especially in case of IgFLNa18-19 and we judged that it would not offer any particularly important new information.

References

Cornilescu, G., Delaglio, F. and Bax, A. (1999) Protein backbone angle restraints from searching a database for chemical shift and sequence homology. J Biomol NMR, *13*, 289–302.

Delsuc, M.A. and Malliavin, T.E. (1998) Maximum Entropy Processing of DOSY NMR Spectra. Analytical Chemistry, *70*, 2146–2148.

Farrow, N.A., Muhandiram, R., Singer, A.U., Pascal, S.M., Kay, C.M., Gish, G., Shoelson, S.E., Pawson, T., Forman-Kay, J.D. and Kay, L.E. (1994) Backbone dynamics of a free and phosphopeptide-complexed Src homology 2 domain studied by 15N NMR relaxation. Biochemistry, *33*, 5984–6003.

Heikkinen, O.K., Permi, P., Koskela, H., Ylänne, J. and Kilpeläinen, I. (2009) 1H, 13C and 15N resonance assignments of the human filamin A tandem immunoglobulin-like domains 16-17 and 18-19. Biomolecular NMR Assignments, in press: DOI 10.1007/s12104-12008-19140-12106.

Heikkinen, S. and Kilpelainen, I. (2001) Linewidth-resolved 15N HSQC, a simple 3D method to measure 15N relaxation times from T1 and T2 linewidths. J Magn Reson, *151*, 314–319.

Herrmann, T., Guntert, P. and Wuthrich, K. (2002) Protein NMR structure determination with automated NOE assignment using the new software CANDID and the torsion angle dynamics algorithm DYANA. J Mol Biol, **319**, 209–227.

Hooft, R.W., Vriend, G., Sander, C. and Abola, E.E. (1996) Errors in protein structures. Nature, *381*, 272.

Kiema, T., Lad, Y., Jiang, P., Oxley, C.L., Baldassarre, M., Wegener, K.L., Campbell, I.D., Ylänne, J. and Calderwood, D.A. (2006) Structure of a filamin-integrin complex reveals the molecular basis of binding and competition with talin. Mol. Cell , *21* , 1–11.

Koskela, H., Kilpelainen, I. and Heikkinen, S. (2004) Evaluation of protein 15N relaxation times by inverse Laplace transformation. Magn Reson Chem, *42*, 61–65.

Lad, Y., Kiema, T.R., Jiang, P., Pentikäinen, O.P., Coles, C.H., Campbell, I.D., Calderwood, D.A. and Ylänne, J. (2007) Structure of three tandem filamin domains reveals auto-inhibition of ligand binding. EMBO J., *26*, 3993–4004.

Laskowski, R.A., Rullmannn, J.A., MacArthur, M.W., Kaptein, R. and Thornton, J.M. (1996) AQUA and PROCHECK–NMR: programs for checking the quality of protein structures solved by NMR. J Biomol NMR, *8*, 477–486.

Nakamura, F., Pudas, R., Heikkinen, O., Permi, P., Kilpeläinen, I., Munday, A.D., Hartwig, J.H., Stossel, T.P. and Ylänne, J. (2006) The structure of the GPIb-filamin A complex. Blood , *107* , 1925–1932.

Pons, J.L., Malliavin, T.E. and Delsuc, M.A. (1996) Gifa V4: a complete package for NMR data-set processing. J. Biomol. NMR, *8*, 445–452.

Schwieters, C.D. and Clore, G.M. (2001) The VMD-XPLOR visualization package for NMR structure refinement. J Magn Reson, *149*, 239–244.

Thompson,J.D., Gibson,T.J., Plewniak,F., Jeanmougin,F. and Higgins,D.G. (1997) The ClustalX windows interface: flexible strategies for multiple sequence alignment aided by quality analysis tools. Nucleic Acids Research, *25*:4876-4882.